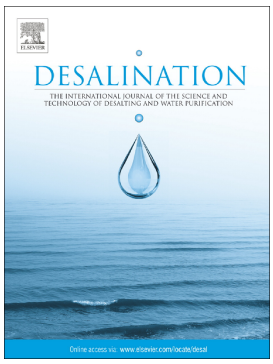

Application of an energy recovery device with RO membrane for wave powered desalination

Tapas K. Das, Matt Folley, Carwyn Frost, Paul Brewster

PII: S0011-9164(24)00775-6

DOI: https://doi.org/10.1016/j.desal.2024.118064

Reference: DES 118064

To appear in: *Desalination*

Received date: 1 May 2024

Revised date: 13 August 2024

Accepted date: 29 August 2024

Please cite this article as: T.K. Das, M. Folley, C. Frost, et al., Application of an energy recovery device with RO membrane for wave powered desalination, *Desalination* (2024), https://doi.org/10.1016/j.desal.2024.118064

Application of an Energy Recovery Device with RO Membrane for Wave Powered Desalination

Tapas K. Das, Matt Folley, Carwyn Frost*

Paul Brewster#

* Marine Research Group, School of Natural and Built Environment, Queen's University Belfast, UK

Pure Marine Gen Ltd, The Innovation Centre, Queen's Road, Belfast, UK

Abstract: A Wave-Driven Desalination System (WDDS) represents an efficient method for harnessing wave energy to facilitate water desalination. Nonetheless, various challenges impede its path to commercial viability. There is a requirement to connect the WDDS to an Energy Recovery Device (ERD), but this is challenging due to the inherent variations in pressure and flow. This unique study demonstrates the working of a small scale WDDS system using a Spiral Wound Reverse Osmosis (SWRO) membrane with a permeate capacity of ~2 m^3/day. The study demonstrates the possibilities to reduce high specific energy consumption (SEC) in WDDS by incorporating a Clark pump as an ERD. The study is the first time an evaluation of an SWRO membrane and Clark pump in-the-loop has been evaluated using variable feed flow and pressure. The utilization of the Clark pump notably reduces SEC to about 3.5 kWh/m^3, which is comparable to that of commercial desalination plants. Furthermore, the Clark pump aids in maintaining a consistent permeate recovery rate of 10% under rectified sinusoidally varying flow conditions – representing the operating conditions more closely to that of practical devices.

Highlights:

1. Demonstration of a small-scale wave driven desalination system (WDDS) with ERD

2. Novel experimental study of an ERD under variable feed flow and pressure
3. Suitability of Clark pump type ERD for small scale WDDS
4. SEC of WDDS with Clark pump is within commercially viable limit

Keywords: wave energy, wave power desalination, WDDS, energy recovery device

Introduction:

In recent decades, research on wave energy conversion has experienced notable advancement, primarily propelled by the imminent peril of climate change stemming from fossil fuel usage. Several wave energy converters (WECs) have been conceived, developed, and subjected to prototype testing. The commercialisation of WEC's has resulted in three broadly accepted device classifications; attenuators, terminators and point-absorbers [1]. Within each of these classification, sub-categories of devices are distinguished. For example, terminators include any device with its principle axis perpendicular to the incident wave direction, such as a wave energy converter based on Salter duck principle [2]. Point-absorbers on the other hand are considered a device which has small body dimensions relative to the wave length [3], such as CorPower device [4]. Similarly, attenuator type devices such as Pelamis wave energy converter showed significant possibilities for wave energy conversion [5].

The fundamental objective underlying the design and implementation of these WECs has been the conversion of wave energy into electrical energy. While generating electrical energy from wave energy remains the key challenge till date, efficient storage of this electrical energy and its integration into existing power grids also pose a significant concern. Consequently, the commercialization of wave energy has encountered limited success in recent years. However, a smaller proportion of commercial developers have identified the application of WEC to sea-water desalination. The technology and resources co-location offers synergy and the energy

density of wave has been recognised for its applicability to hydraulic power-take-offs and high pressure, low flow rate systems, similar in requirement to RO desalinisation.

The Wave Driven Desalination System (WDDS) integrates a wave energy converter directly with a reverse osmosis membrane, facilitating the production of fresh water from seawater. This system harnesses pressure energy derived directly from the Wave Energy Converter (WEC), eliminating the intermediate conversion of wave energy into electricity [6]. Consequently, the WDDS represents a more efficient utilization of abundant wave energy when compared to conventional methods-such as conversion of wave energy to electrical energy and then subsequent conversion of mechanical and hydraulic energy to generate fresh water.

Folley et al [7] developed numerical studies for a WDDS with a hypothetical OWSC feeding an array of RO membranes with a ~35% recovery ratio. Further consideration of this work by Yu and Jenne [8] found close agreement using the WEC-Sim model applied on NREL reference model-RM5 directly driving a SWRO with pressure-exchanger. Recent publication by Brodersen et al [9] considered a hypothetical WDDS for batch reverse osmosis (BRO) using an OWSC, 50% recovery ratio and flow control device on the turbine side of the PTO to smooth out wave-to-wave fluctuations.

Sitterley et al [10] investigated the impact of pressure fluctuations from a hypothetical directly driven wave energy converter using an experimental setup including a high-head pump driving the feed flow through a RO membrane with an actuator needle valve fluctuating to vary the back-pressure in the system. Conductivity, flow, and pressure are measured for feed, brine and permeate lines. Sitterley et al.'s study involved a simple sinewave oscillation in feed pressure at various amplitudes and frequencies and showed no detrimental impact on membrane integrity from sinusoidal fluctuations, and longer wave lengths resulted in lower salinity permeate. Whilst,

Das et al. [11], undertook a similar study with a rectified sinewave oscillation, more closely representing the output profile from a WEC's hydraulic PTO. The findings showed similar behaviour in membrane performance to Sitterly et al. However, the study by Das et al. showed significant degradation of the RO membrane (reduced salt rejection) when subjected to variable feed flow and pressure for long time.

Recent publication by Mi et al [12] demonstrated a model scale OWSC directly driving a RO system. The experimental setup used an accumulator between the double-acting piston and RO membrane to smooth pressure fluctuations and a needle valve in the brine line, after the RO membrane to set the back pressure of the system, no energy recovery device was used.

Commercially, one company Pure Marine Gen features a floating WEC technology, the DUO, which simultaneously captures power from heave and pitch/ surge motion. A small wave driven desalinisation system named the DUO-DS was developed for the U.S. Department of Energy 'Waves to Water Prize' [13] and is shown in Fig. 1. The device has a 4m diameter surface float connected to a submerged tank reacts against the float through tension cables. The DUO-DS utilises a hydraulic PTO to pressurise seawater into a SWRO system. The device features three double-acting hydraulic rams, actuated by the relative motion of the float and plate under wave conditions, in a similar manner to the illustration in Fig. 1. This actuation pressurises water to a common feed for the SWRO system. The prototype can produce 2 m^3/day depending on the wave resource at the deployment site and was successfully deployed and monitored in 2021 at a shallow water site near Strangford Lough, Northern Ireland.

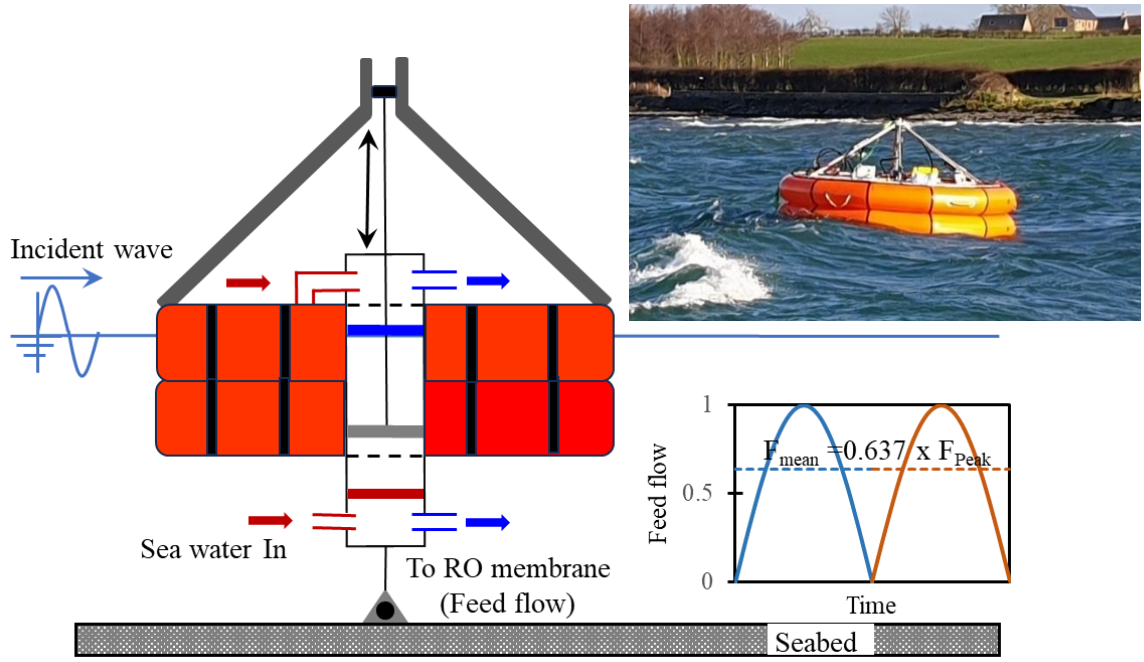

Fig. 1 Schematic of the relative motion and piston actuation; Inset: Sea trials of Prototype DUO-DS in Strangford Lough, 2021

However, there is a significant challenge inherent in this system. The WDDS is subjected to variable feed flow and pressure conditions, in contrast to the standard reverse osmosis membranes designed for constant flow and pressure. So that the WDDS faces a challenge in recovering useful energy from the waste brine water. While conventional desalination plants employ energy recovery devices to reclaim pressure energy, no study to date has documented the performance of an energy recovery device under realistic variable feed flow and feed pressure conditions.

Energy Recovery Device:

Desalination from sea water is a highly energy intensive process. Nassrullah et al.[14] has given a detailed analysis of energy requirements for various types of desalination processes.

Desalination systems typically produce high-pressure rejected brine, comparable to the feed pressure, resulting in a significant loss of pressure energy if left unused. To address this issue, the concept of Energy Recovery Devices (ERDs) has emerged, aiming to harness the pressure energy of the brine and utilize it to augment the pressure of the feed flow. This approach has the potential to substantially reduce specific energy consumption by 40-60% [15]. In the early stages, Pelton wheels were commonly employed as ERDs in desalination units. However, in recent times, isobaric units have gained prominence, primarily due to their capacity to mitigate losses associated with mechanical rotating components of Pelton wheels. Isobaric chambers have demonstrated impressive efficiency levels of up to 97% [16], making them a preferred choice for modern desalination systems. A more detailed analysis on reduction of SEC over the years by using new technologies can be found in [14,17–20].

The isobaric chambers are one of the popular ERDs to be used commercially. These can be categorized into two distinct groups: positive displacement types and rotary displacement types. The positive displacement type ERDs are equipped with either two or three isobaric chambers, housing a piston that facilitates pressure transfer. An example of a positive displacement type isobaric chamber ERD is the DWEER™ [21]. In contrast, rotary displacement type ERDs encompass a solitary chamber, featuring an automatic rotation of a cylindrical rotor driven by the flow of high-pressure brine. Notably, this configuration lacks any valves or pistons, resulting in a marginally higher pressure exchange efficiency compared to the positive displacement type ERDs. A prominent example of this ERD variant is the PX™ pressure exchanger manufactured by Energy Recovery Inc. [15,22,23].

It is noteworthy that the type of Energy Recovery Device (ERD) required for a desalination system is highly dependent on the plant's capacity. The commercially available ERDs were

primarily developed for large-scale desalination plants. An extensive review by Kim et al.[24] illustrates the application of various ERD types in commercial plants worldwide. The most frequently used ERDs are the pressure exchanger type ERD PX™ and the positive displacement type isobaric chamber ERD DWEER™. The desalination plants examined in this review are large-scale facilities with capacities exceeding 10,000 m³/day. However, a wave driven desalination system is fundamentally a small-scale desalination system compared to such commercial plants. Consequently, the use of conventional ERDs is not viable within a WDDS framework.

An alternative approach is the utilization of pressure intensifiers, whereby the brine pressure directly transfers to the feed flow through a mechanical system. Examples of pressure intensifiers include the axial piston pump (APP) and axial piston motor (APM) developed by Danfoss [25], as well as the Clark pump manufactured by Spectra Watermakers Inc. [26,27]. These pressure intensifiers are often well-suited for low-capacity desalination plants. Unlike pressure exchangers, they eliminate the need for a booster pump; however, they usually have a fixed recovery ratio. A commercially available SWRO and Clark pump is reported to produce ~1.25 m^3/day of permeate [28], to increase this capacity parallelisation of the system components would be required, making it a capital intensive solution for high-capacity (utility scale desalinisation). Consequently, employing such ERDs in a full-scale desalination plant could reduce flexibility. Nonetheless, a primary advantage of utilizing the Clark Pump with WDDS is its ability to function without the need for additional electrical energy. Most commercially available ERDs, such as the DWEER™, PX™, and Danfoss APP, require an auxiliary booster pump for operation. In contrast, the Clark Pump is entirely mechanical, allowing the required feed pressure to be adjusted by altering the piston size of the pump. This feature makes the Clark

Pump the most suitable option for a WDDS compared to other available ERDs.

Figure 2 presents a schematic of the Clark Pump (CP), which is a reciprocating pressure intensifier. Developed for the maritime market as a water maker by Clark Permar in association with Spectra Watermakers Inc [28]. The single most important attribute to a Clark pump is the difference in effective areas on the outside and inside faces of the pistons. The inside faces of the pistons have a reduced area due to the connecting rod, this creates an area ratio, which is significant for the pressure differential, it also creates a volume ratio between the chambers. Being a reciprocal device an analytical expression for an idealised device can be understood from the pistons moving in one direction.

Concentrating on the CP's opposing cylinders chamber, continuity dictates that:

$$Q_f = \frac{Q_e}{1-R_t} = \frac{Q_c}{1-R_t} = Q_h \quad (1)$$

Where the feed flow (Q_f) and high-pressure flow (Q_h) are equal to a factor of the exhaust flow (Q_e) and concentrate flow (Q_c). Whereby the recovery ratio (R_t) is the area ratio between the inside and outside areas of the opposing pistons.

$$R_t = \frac{A_{Pi}}{A_r} \quad (2)$$

Where the piston area and rod area are design variables, Spectra offers a range of CP's with recovery ratios spanning from 7 - 20%.

Rearranging equation (1) to make R_t the subject results in:

$$R_t = \frac{Q_f - Q_c}{Q_f} \quad (3)$$

Whereby:

$$Q_p = Q_f - Q_c \quad (4)$$

Thus, the area ratio of the piston in an ideal CP will dictate or fix the permeate flow (Q_p) as a

ratio of the feed flow, setting a constant recovery ratio.

$$R_t = \frac{A_{Pi}}{A_r} = \frac{Q_p}{Q_f} \quad (5)$$

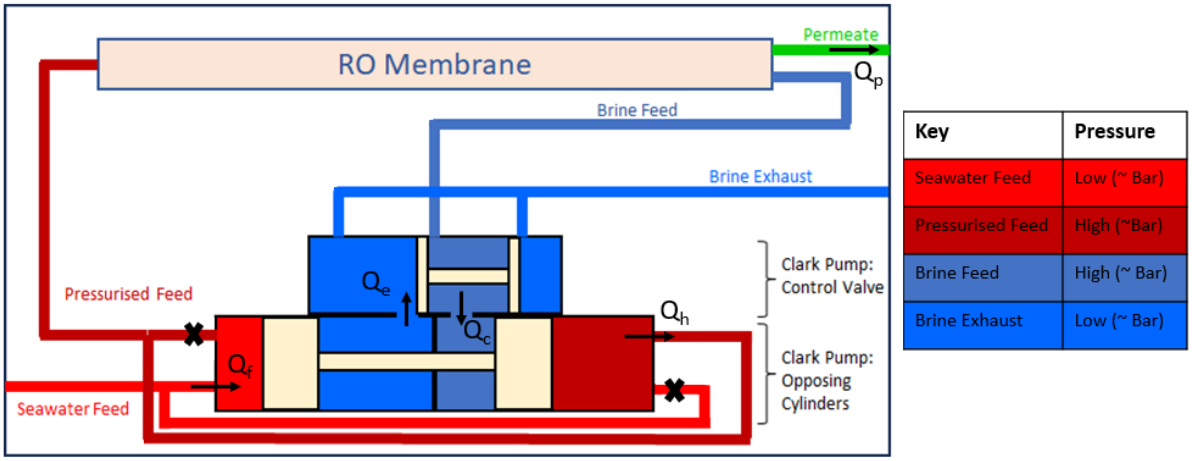

Fig. 2 A schematic showing pressure intensifier type ERD (Clark pump)

Previous investigations have explored the effectiveness of the Clark pump under various conditions. However, the number of articles related to Clark pump is limited, mainly because of its suitability for low-capacity systems only. Table 1 reports the articles related to Clark pump, with its production capacity and the specific energy consumption of the system.

Table 1 Review of SWRO coupled with Clark pump type ERD

Authors	Production Capacity	SEC (kWh/m^3)
Thomson et al. [27]	460 l/h	~3.5
Mohamed et al. [29]	2.6 m^3/d	~3
Thomson & Infield [30]	1.47 m^3/d	~4
Mohamed et al. [31]	1.7 m^3/d	~3.3
Manolakos et al. [32]	0.1 m^3/h	~3.8-6

Bermudez-Contrers & Thomson [33]	1 m^3/d	~3.5-4.5
Dimitriou et al. [34]	83 l/h	~5.7

.

Manolakos et al. [32] conducted an experimental study to assess the economic viability of a Clark pump within a solar PV-RO desalination system with a capacity of 0.1 m^3/hr. The reported specific energy consumption (SEC) of this system ranged from 3.8 to 6 kWh/m^3. Likewise, Thomson and Infield [30] conducted a laboratory demonstration of photovoltaic-powered reverse osmosis desalination, achieving an SEC of less than 4 kWh/m^3 for a wide range of operations. In a different study, Mohamed et al. [29] experimentally investigated the performance of a Clark pump in a system with a capacity of 2.6 m^3/d, reporting a SEC of 3 kWh/m^3 while utilizing the Clark pump. Similarly, Thomson et al. [27] conducted a numerical and experimental study of a desalination system incorporating the Clark pump, revealing a comparable SEC of 3.5 kWh/m^3.

The literature review search parameters included all studies using a Clark pump and SWRO for seawater desalinisation. It is noted that all studies used the Clark pump with constat feed flow only. No study has mentioned the use of Clark pump under variable feed flow.

Research Objective:

This research is the first time an experimental study of an SWRO and Clark Pump ERD have been tested with fluctuating feed flow and pressure. As highlighted by reviewing existing literature all preceding investigations related to Clark pump ERD maintained a constant feed flow and feed pressure throughout their studies. Nevertheless, in the context of a wave-driven desalination system, both the feed flow and pressure will fluctuate in response to the wave profile. This unique research examines the efficacy of a SWRO and Clark pump in-the-loop under dynamic conditions of varying feed flow and pressure. Additionally, this study addresses

the economic feasibility of integrating an energy recovery device within the context of a wave-driven desalination system. Fig. 3. Shows a flow chart of the present experimental study.

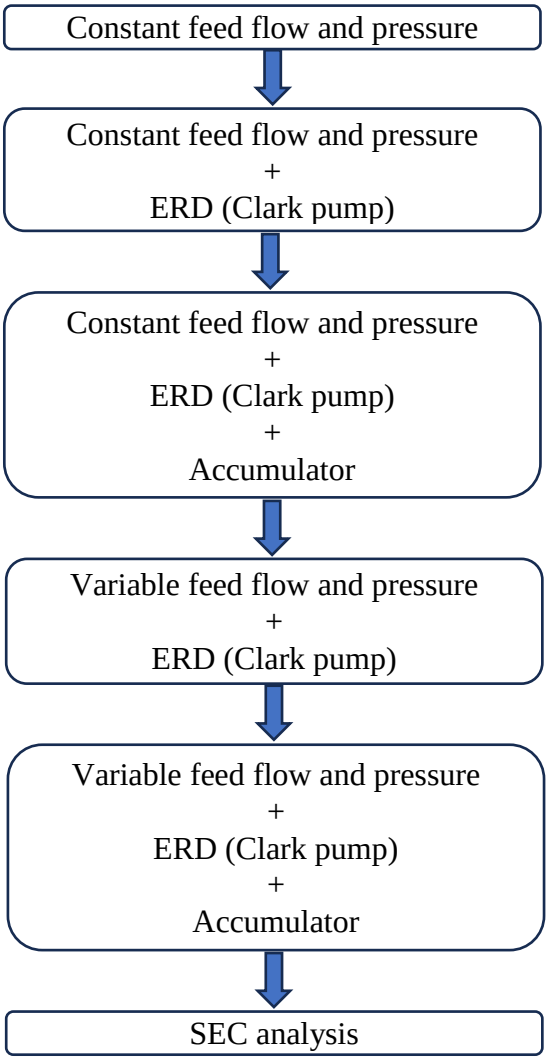

Fig. 3 Flow chart of the experimental procedure

Experimental set up:

Figure 4 (a) shows the preliminary experimental setup for testing the RO membrane with steady flow and pressure to create a benchmark for comparison with subsequent tests. The experimental setup consists of a water tank which contains the feedwater with equivalent salinity of seawater.

A high-pressure pump is used to supply the feedwater to the RO module with required flow and pressure. After passing through the RO module, the feed water is separated into high retentate (brine water) and permeate (clean water). The actuated needle valve in the retentate line helps to maintain the feed pressure as well. The pressure sensors, flow sensors and conductivity sensors are deployed at different points to measure the pressure, flow and salinity, respectively. As the high-pressure water circulates within the experimental setup in a closed loop, the water temperature increases gradually. An air-cooled chiller is used to keep the temperature constant within the experiment setup. A Filmtec™ SW30-2521 membrane is used for the experiment with an active membrane area of 1.2 m^2. Further details about the experimental setup and error analysis are discussed in the previous publication [11] and not repeated here for the brevity of the article.

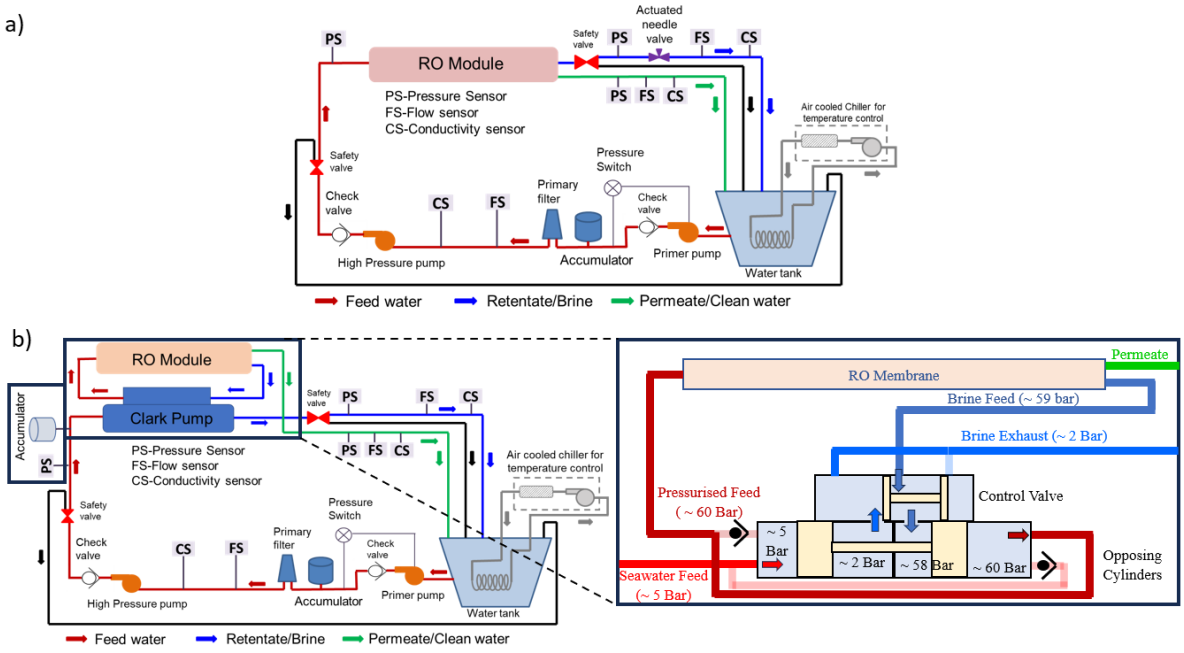

Fig. 4 Schematic Arrangement of the experimental set-up a) RO module only b) RO and Clark Pump with and without an accumulator

Performance of the membrane under constant flow and pressure:

The RO membrane underwent initial testing under conditions of constant flow and pressure to establish a set of baseline values for subsequent experiments. During this phase, the RO membrane was subjected to a constant feed flow ranging from 6L/min to 14 L/min, with increments of 2 L/min, and the feed pressure was systematically adjusted from 35 Bar to 60 Bar, with increments of 5 Bar. The determination of the lower limit was based on the osmotic pressure of seawater, while the upper limit was established in consideration of the safe operating threshold of the test setup.

Each combination of flow and pressure conditions required the continuous operation of the system for approximately 30 minutes until the permeate flow and salinity values stabilized. Once stability was achieved, data recording occurred for a 5-minute duration. Figure 5 illustrates the variations in permeate recovery and permeate salinity in relation to feed pressure and feed flow. The plots depict average values over a 5-minute period, and the error bars indicate the corresponding uncertainty.

Fig. 5 (a) & (c) reveal that at lower feed pressure, near the osmotic pressure, permeate recovery is relatively independent of the feed flow rate. However, at a constant feed pressure, the percentage of permeate recovery gradually decreases with an increase in feed flow rate. This phenomenon is attributed to the reduced interaction time between water molecules and the membrane at higher feed flow rates, resulting in decreased permeate production. Fig. 5(b) demonstrates that for any constant feed flow rate, an increase in feed pressure leads to a significant decrease in permeate salinity. Particularly, as the feed pressure increases, the permeate salinity decreases rapidly. This rate of decrease becomes more gradual at higher feed pressure values, as illustrated in Fig. 5(d). It is essential to note that the observed behaviour of

the RO membrane aligns with the characteristics expected of a standard RO membrane used in seawater desalination.

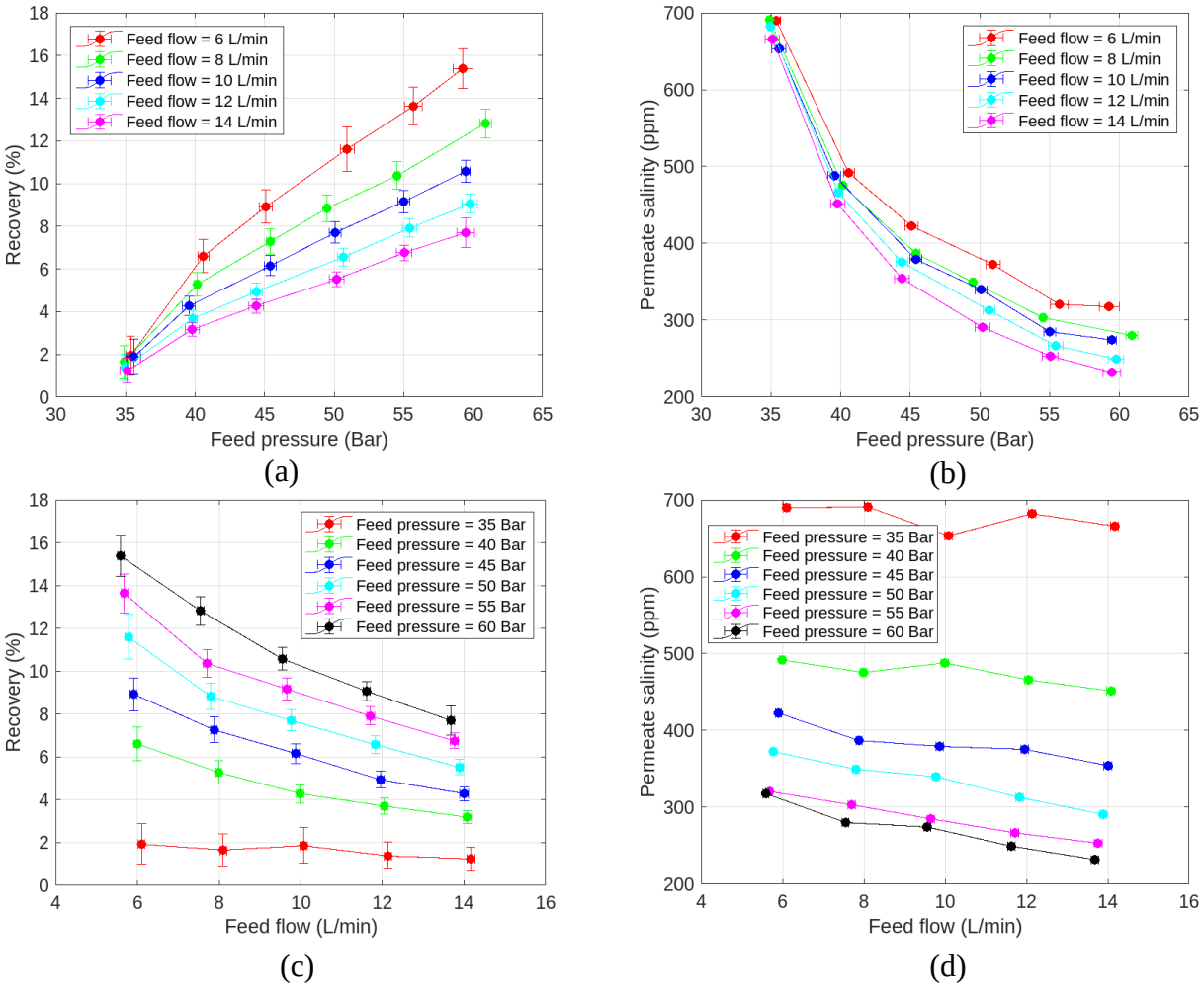

Fig. 5 Variation of permeate recovery and permeate salinity with respect to (a), (b) feed pressure and (c), (d) feed flow

RO membrane with Clark pump-constant flow and pressure:

In the following phase, the RO membrane underwent testing in conjunction with a Clark pump positioned at its inlet. The specific connections involving the Clark pump (CP) are detailed in Fig. 4 (b). (without accumulator). Notably, the actuated needle valve is omitted from the system

configuration when employing a CP. A steady feed flow is introduced into the CP, wherein it undergoes pressurization by the high-pressure brine discharged from the RO membrane. Functioning cyclically, the CP delivers high-pressure water to the RO membrane in each cycle. It is worth noting that the pressure values depicted in the figure are approximate and vary with the feed flow rate. Fig. 4 (b) shows the balance of pressures across the four chambers of the Clark pump. With the low pressure seawater feed at ~5 bar and the high pressure brine at ~58 bar entering the chambers expanding them and compressing the low pressure brine exhaust at ~2 bar and the resulting in a high pressure feed ~60 bar to the RO membrane.

Figure 6 provides a comparative analysis of permeate recovery and permeate salinity in the presence of the CP. The feed flow rate was varied whilst the feed pressure was maintained at approximately 5 bar. Notably, the Clark pump maintains permeate recovery at a ~10% with marginal reduction in response to increasing the feed flow velocity. This agrees with the investigations of Thomson [35] which showed a relatively small reduction in efficiency in response to an increasing feed pressure (~ 3%), and a slightly greater reduction in efficiency in response to an increase feed flow (~ 7%). Moreover, the utilization of the Clark pump results in a significant reduction in permeate salinity, particularly at higher feed flow rates.

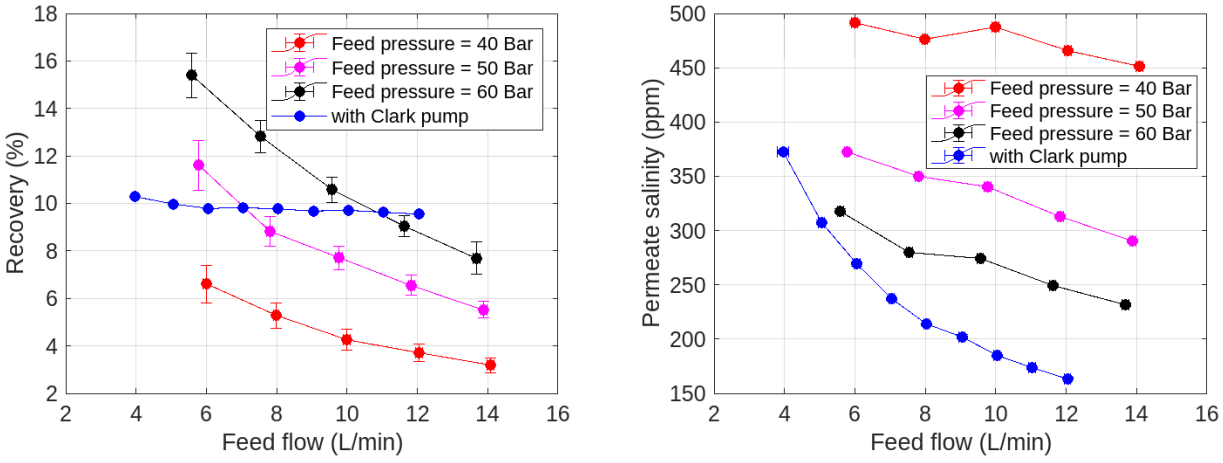

Fig. 6 Comparison of permeate recovery & salinity with and without Clark pump

RO membrane with Clark pump & accumulator-constant flow and pressure:

In the subsequent stage, an accumulator is introduced preceding the entrance of the Clark pump, as illustrated in Fig. 4 (b) (with accumulator). Subsequently, the feed flow traverses through the accumulator before reaching the Clark pump. Permeate recovery and salinity values are assessed across various flow rates and compared with values from prior experiments conducted without an accumulator and Clark pump (CP).

Figure 7 indicates that the utilization of an accumulator does not alter either permeate recovery or salinity. However, an intriguing phenomenon demonstrates in the feed pressure when not employing the accumulator, as depicted in Fig. 8. As the Clark pump operates in cycles, there is a sudden surge in feed pressure when the piston transitions from one end to the other. This abrupt pressure surge translates into a palpable jerk within the Clark pump, necessitating an enhanced support structure for the pump within the experimental setup. Moreover, this phenomenon may introduce sudden imbalances within a system employing the Clark pump, particularly in a model Wave-driven desalination system (WDDS). Nonetheless, as illustrated in Fig. 8, the accumulator effectively mitigates sudden pressure surges, facilitating smooth system operation. This efficacy stems from the accumulator's ability to maintain feed water at a consistent pressure while the piston within the Clark pump undergoes directional changes, thereby preventing abrupt pressure fluctuations at the pump's inlet.

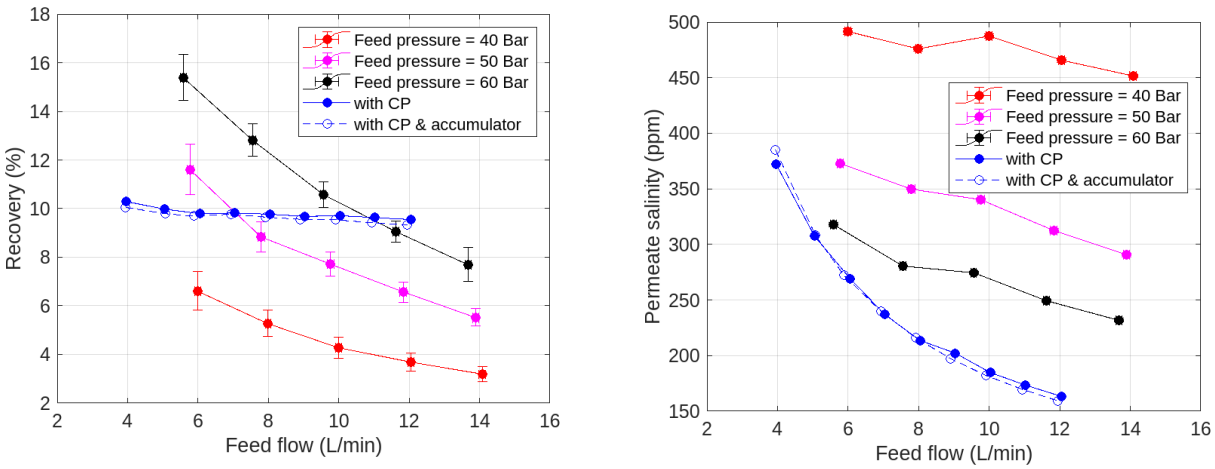

Fig. 7 Comparison of permeate recovery & salinity with and without accumulator

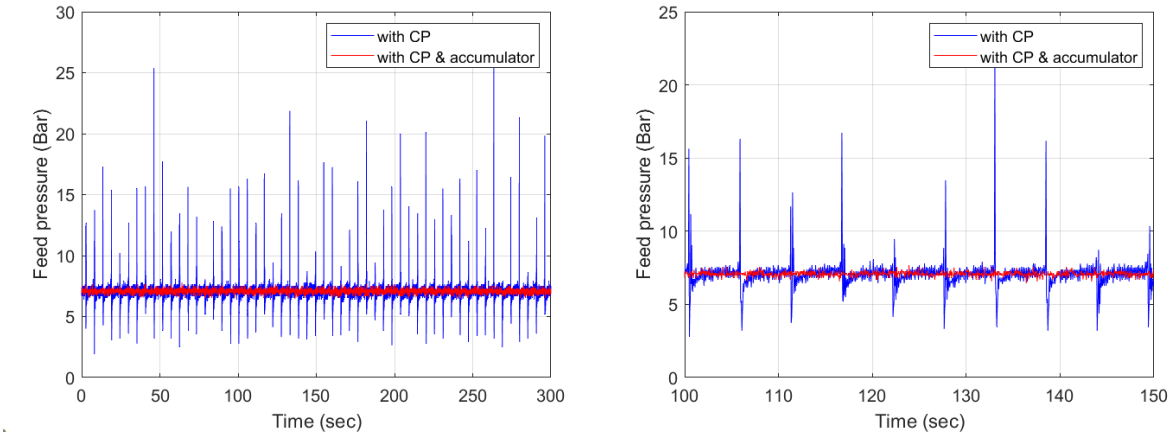

(a) (b)

Fig. 8 (a) Comparison of feed pressure with and without accumulator (b) a zoomed view

RO membrane with Clark pump -varying flow and pressure

The following section presents the findings resulting from subjecting the RO membrane to rectified sinusoidally varying flow in conjunction with a Clark pump. The rectified nature of the flow best describes the nature of the flow from a double-acting piston as described in previous research [11]. The RO membrane underwent testing across five distinct mean flow conditions, ranging from 4 L/min to 8 L/min. To maintain consistent mean flow conditions during rectified

sinusoidally varying flow, corresponding peak flow rates were set for each mean flow, as outlined in Table 2. Tests were conducted across varying time periods (T_p), spanning from 7.5 seconds to 30 seconds.

Figure 9 depicts the permeate recovery and permeate salinity for different flow conditions under the application of rectified sinusoidally varying flow. Notably, the permeate recovery remained approximately constant at 10%, mirroring the outcomes achieved under constant flow conditions. Additionally, permeate salinity was found to correlate solely with the mean flow rate, decreasing as mean flow rate increased. However, it is noteworthy that permeate salinity exhibited independence from the time period of rectified sinusoidally varying flow.

Table 2 Experimental conditions for rectified sinusoidally varying flow

Peak Flow (L/min)	Mean flow (L/min)	Time periods (sec)
6.4	4	7.5,10,12.5,15,30
7.84	5	
9.42	6	
11	7	
12.55	8	

.

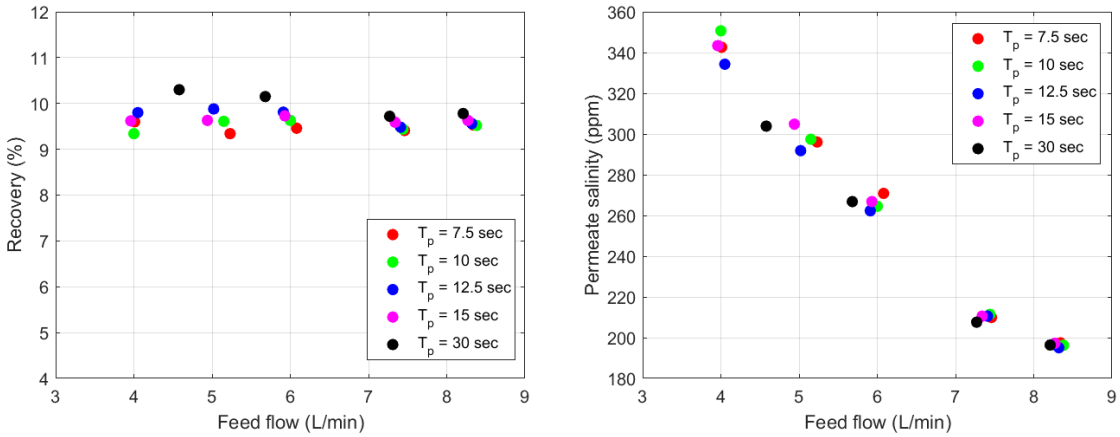

Fig. 9 Permeate recovery & salinity for different mean feed flow and time period

RO membrane with Clark pump and accumulator -varying flow and pressure

In the subsequent phase, the accumulator was reintroduced into the system configuration, positioned prior to the Clark pump, enabling the rectified sinusoidally varying flow to traverse through the accumulator before reaching the Clark pump. Table 3 presents the various mean flow rates and corresponding time periods utilized in this setup. Analysis of Fig. 10 indicates that the accumulator exerts minimal influence on both permeate recovery and permeate salinity values. This outcome parallels the observations made during testing under constant feed flow and pressure conditions. Once more, it is noted that permeate recovery and salinity remain unaffected by the time period of flow, underscoring their independence from this variable.

Table 3 Experimental conditions for rectified sinusoidally varying flow

Peak Flow (L/min)	Mean flow (L/min)	Time periods (sec)
6	3.81	
6.4	4	
7	4.45	

7.84	5	5,7.5,10,12.5,15,30
8	5.1	
9	5.73	
9.42	6	
10	6.37	
11	7	
12	7.64	
12.55	8	

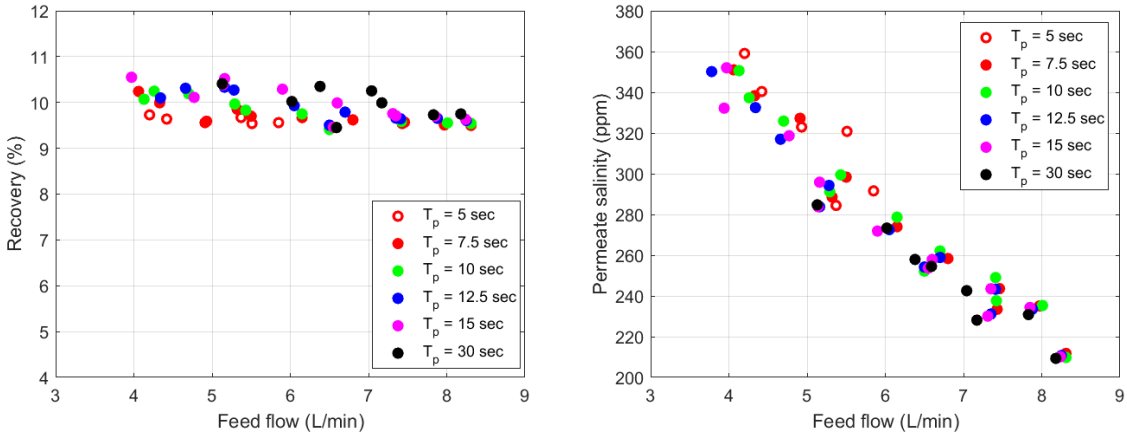

Fig. 10 Permeate recovery & salinity for different mean feed flow and time period

Permeate flow analysis under rectified sinusoidal flow:

To further investigate the impact of the Clark pump and accumulator on permeate flow, two distinct cases are examined. In the first case, analysis focuses on permeate flow under identical mean flow (6.4 L/min) and peak flow (10 L/min) conditions, but varying time periods (T_p), as depicted in Fig. 11(a). The inverse peaks in the figure correspond to instances when the Clark pump piston reverses direction. Remarkably, it is observed that time period variations exert no

noticeable influence on either permeate flow rate or piston movement within the Clark pump.

In the second case, permeate flow analysis is conducted across three different mean flow rates (4, 6, and 8 L/min), with a fixed time period of 10 seconds, as illustrated in Fig. 11(b). A notable disparity is evident compared to the preceding case. Specifically, higher mean feed flow rates yield elevated permeate flow rates while maintaining a consistent 10% permeate recovery across all scenarios. However, a greater occurrence of inverse peaks is observed with higher mean feed flow rates. This phenomenon arises due to the accelerated filling of the cylinder inside the Clark pump with increasing mean feed flow rates, consequently prompting more rapid changes in piston direction. Subsequently, the 10% recovery rate is sustained across all mean feed flow rates.

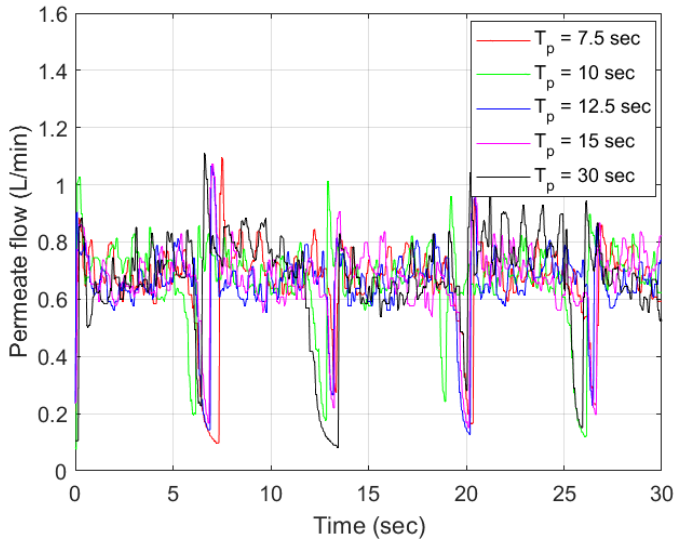

Fig. 11(a) Permeate flow for same mean flow and different time periods

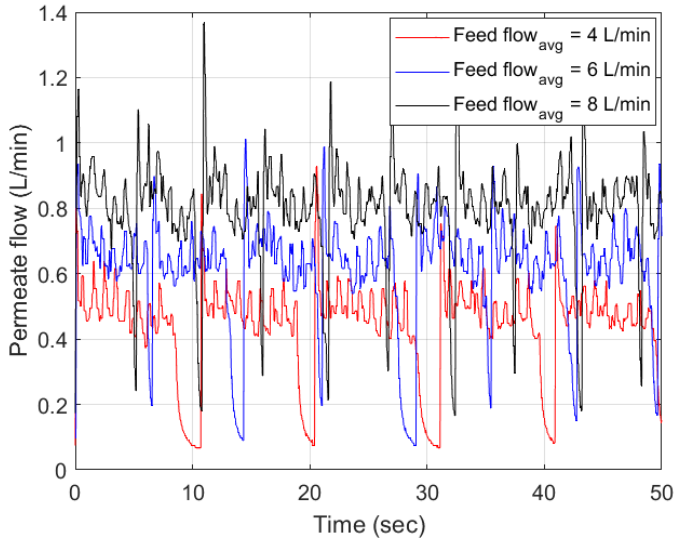

Fig. 11(b) Permeate flow for different mean flow and same time period

Specific Energy Consumption:

Figure 12 illustrates a comparison of specific energy consumption across various test scenarios with and without the energy recovery device. The vertical axis, from left to right, represents the mean feed flow rate, mean feed pressure, permeate recovery percentage, and specific energy consumption, respectively. The black lines depicted in the figure denote conditions lacking the energy recovery device. Whereas, the blue lines depict the scenario with energy recovery device. In instances where the test setup operates without the energy recovery device, the feed pressure consistently exceeds the osmotic pressure necessary for effective functioning of the RO membrane, across different feed flow rates. Depending on variations in feed flow and pressure, permeate recovery spans a wide range, from 3% to 15%. Correspondingly, specific energy consumption fluctuates between approximately 10 to 36 kWh/m^3.

Conversely, utilization of the Clark pump yields notably lower feed pressures, ranging between 5 and 10 bar. Consequently, this substantially reduces the specific energy consumption to

approximately 2-3.5 kWh/m^3, aligning closely with commercial desalination plants. Moreover, with the Clark pump, permeate recovery consistently maintains a level near 10% across all feed flow conditions.

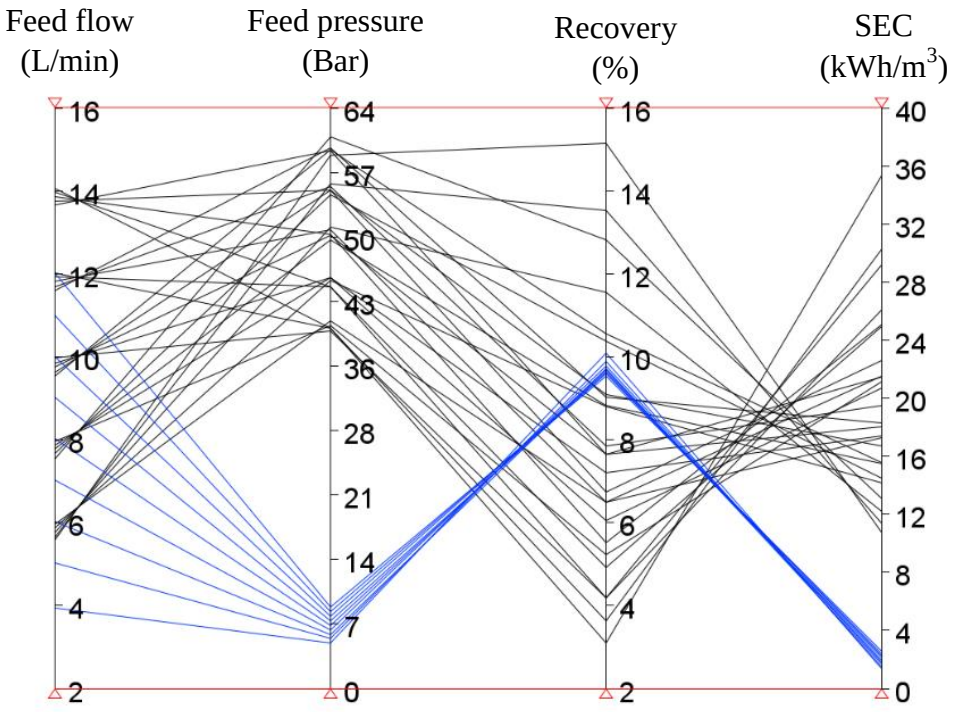

Fig. 12 Specific energy consumption for different feed flow rates: Black lines are for tests without ERD and blue lines are with ERD

Conclusion:

The present study is the first time a systematic experimental investigation of a reverse osmosis membrane, both with and without the integration of an energy recovery device, under conditions of steady and variable flow representative of a wave driven desalinisation system has been undertaken. A Clark pump energy recovery device was employed in the experimental setup. Initially, the RO membrane underwent testing solely under steady flow and pressure conditions to establish a baseline for comparison. Subsequent tests were conducted under rectified

sinusoidally varying flow conditions, with modifications made to the experimental setup to accommodate a Clark pump and an accumulator.

The findings demonstrate that the inclusion of a Clark pump facilitates a constant permeate recovery at user-defined levels (in this instance, 10%), irrespective of fluctuations in flow rate or pressure. Moreover, the integration of an accumulator was observed to mitigate pressure surges generated by the Clark pump, thereby facilitating smooth system operation with no significant detriment to performance. Further work to investigate the lifecycle costs and maintenance periods of such a WDDS is required and will be the subject of further work.

The incorporation of the Clark pump markedly reduces the system's specific energy consumption (SEC), reducing it to below ~3.5 kWh/m^3, aligning with previous experimental findings [27,30,32,36]. Conversely, it imposes limitations on permeate recovery. However, for small-scale wave-powered desalination units, maintaining a low SEC rate assumes greater significance for the commercial feasibility of such systems. Nonetheless, achieving a harmonious equilibrium between permeate recovery and SEC is imperative for the successful commercialization of a wave-driven desalination system.

Furthermore, it is crucial to gain a deeper understanding of the RO membrane's behaviour under varying flow and pressure conditions. Two areas of further research are under development:

1. Life-cycle assessment of a SWRO and Clark pump subject to variable feed flow and pressure.
2. Performance standards for wave-driven desalinisation systems – unlike electricity generation (for which WEC’s have power performance standards) a WDDS requires a standard to certify the quality and quantity of water produced for a given sea-state.

Working with Pure Marine Gen, these research challenges are vital for the commercialisation of

wave-driven desalinisation.

Acknowledgement:

This work was supported by the EPSRC, ORE Supergen, *DesWEC* flex fund project [FF2020-1012] and CASE funded *DUO-DS* project [A1130].

Acknowledgement of the technical contribution of Mr Ian Benson and Mr Kamil Kanas for the design power electronic and control components. Also, to the technician support received from Mr Desmond Hill and Mr Daniel Reid in fabrication and maintaining of the experimental apparatus and associated components.

CRediT author statement

Tapas K. Das: Methodology, Software, Validation, Formal analysis, Investigation, Data Curation, Writing - Original Draft, Writing - Review & Editing, Visualization **Matt Folley:** Conceptualization, Methodology, Formal analysis, Writing - Review & Editing, Supervision, Funding acquisition **Carwyn Frost:** Methodology, Resources, Writing - Review & Editing, Supervision, Project administration, Funding acquisition. **Paul Brewster:** Methodology, Resources, Writing - Review & Editing, Supervision, Funding acquisition

Bibliography:

[1] Gallutia D, Tahmasbi Fard M, Gutierrez Soto M, He JB. Recent advances in wave energy conversion systems: From wave theory to devices and control strategies. Ocean Eng 2022;252:111105. https://doi.org/10.1016/J.OCEANENG.2022.111105.

[2] Pecher A, Kofoed JP, Larsen T, Marchalot T. Experimental Study of the WEPTOS Wave Energy Converter. Proc. ASME 2012 31st Int. Conf. Ocean. Offshore Arct. Eng. OMAE2012 July 1-6, 2012, Rio Janeiro, Brazil, 2012, p. 1–10.

[3] Budar K, Falnes J. A resonant point absorber of ocean-wave power. Nature

1975;256:478–9. https://doi.org/10.1038/256478a0.

[4] Todalshaug JH, Ásgeirsson GS, Hjálmarsson E, Maillet J, Möller P, Pires P, et al. Tank testing of an inherently phase-controlled wave energy converter. Int J Mar Energy 2016;15:68–84. https://doi.org/10.1016/j.ijome.2016.04.007.

[5] Yemm RW, Henderson RM, Taylor CAE. The OPD Pelamis WEC: Current status and onward programme. Proc. 4th Eur. Wave Energy Conf. Alborg Denmark., 2000. https://doi.org/10.1080/01430750.2003.9674899.

[6] Lotfy HR, Staš J, Roubík H. Renewable energy powered membrane desalination — review of recent development. Environ Sci Pollut Res 2022;29:46552–68. https://doi.org/10.1007/s11356-022-20480-y.

[7] Folley M, Peñate Suarez B, Whittaker T. An autonomous wave-powered desalination system. Desalination 2008;220:412–21. https://doi.org/10.1016/J.DESAL.2007.01.044.

[8] Yu Y-H, Jenne D. Analysis of a Wave-Powered, Reverse-Osmosis System and Its Economic Availability in the United States: Preprint 2017.

[9] Brodersen KM, Bywater EA, Lanter AM, Schennum HH, Furia KN, Sheth MK, et al. Direct-drive ocean wave-powered batch reverse osmosis. Desalination 2022;523:115393. https://doi.org/10.1016/J.DESAL.2021.115393.

[10] Sitterley KA, Cath TJ, Jenne DS, Yu YH, Cath TY. Performance of reverse osmosis membrane with large feed pressure fluctuations from a wave-driven desalination system. Desalination 2022;527:115546. https://doi.org/10.1016/J.DESAL.2022.115546.

[11] Das TK, Folley M, Lamont-Kane P, Frost C. Performance of a SWRO membrane under variable flow conditions arising from wave powered desalination. Desalination 2023:117069. https://doi.org/10.1016/J.DESAL.2023.117069.

[12] Mi J, Wu X, Capper J, Li X, Shalaby A, Wang R, et al. Experimental investigation of a reverse osmosis desalination system directly powered by wave energy. Appl Energy 2023;343:121194. https://doi.org/10.1016/J.APENERGY.2023.121194.

[13] News Release: DRINKing It in: Five Teams and Their Desalination Designs Earn a Spot in Final Stage of Waves to Water Prize Competition | News | NREL n.d. https://www.nrel.gov/news/press/2021/drinking-it-in-five-teams-and-their-desalination-designs-earn-a-spot-in-final-stage-of-waves-to-water-prize-competition.html (accessed March 19, 2024).

[14] Nassrullah H, Anis SF, Hashaikeh R, Hilal N. Energy for desalination: A state-of-the-art review. Desalination 2020;491. https://doi.org/10.1016/j.desal.2020.114569.

[15] Stover RL. Development of a fourth generation energy recovery device. A "CTO's Notebook." Desalination 2004;165:313–21. https://doi.org/10.1016/j.desal.2004.06.036.

[16] Arenas Urrea S, Díaz Reyes F, Peñate Suárez B, de la Fuente Bencomo JA. Technical review, evaluation and efficiency of energy recovery devices installed in the Canary Islands desalination plants. Desalination 2019;450:54–63. https://doi.org/10.1016/j.desal.2018.07.013.

[17] Yagnambhatt S, Khanmohammadi S, Maisonneuve J. Reducing the specific energy use of seawater desalination with thermally enhanced reverse osmosis. Desalination 2024;573. https://doi.org/10.1016/j.desal.2023.117163.

[18] Yin F, Kong X, Zhang Y, Ma Z, Nie S, Ji H, et al. Numerical study on the energy consumption characteristics of a novel integrated pump-motor unit for SWRO desalination system. Desalination 2023;554:116514. https://doi.org/10.1016/j.desal.2023.116514.

[19] Lim YJ, Ma Y, Chew JW, Wang R. Assessing the potential of highly permeable reverse

osmosis membranes for desalination: Specific energy and footprint analysis. Desalination 2022;533:115771. https://doi.org/10.1016/j.desal.2022.115771.

[20] Bundschuh J, Kaczmarczyk M, Ghaffour N, Tomaszewska B. State-of-the-art of renewable energy sources used in water desalination: Present and future prospects. Desalination 2021;508. https://doi.org/10.1016/j.desal.2021.115035.

[21] Schneider B. Selection, operation and control of a work exchanger energy recovery system based on the Singapore project. Desalination 2005;184:197–210. https://doi.org/10.1016/j.desal.2005.04.031.

[22] Eshoul NM, Agnew B, Al-weshahi MA, Atab MS. Exergy Analysis of a Two-Pass Reverse Osmosis (RO) Desalination Unit with and without an Energy Recovery Turbine (ERT) and Pressure Exchanger (PX) 2015:6910–25. https://doi.org/10.3390/en8076910.

[23] Cameron IB, Clemente RB. SWRO with ERI ' s PX Pressure Exchanger device — a global survey 2008;221:136–42. https://doi.org/10.1016/j.desal.2007.02.050.

[24] Kim J, Park K, Yang DR, Hong S. A comprehensive review of energy consumption of seawater reverse osmosis desalination plants. Appl Energy 2019;254:113652. https://doi.org/10.1016/j.apenergy.2019.113652.

[25] Valbjørn A. ERD for small SWRO plants. Desalination 2009;248:636–41. https://doi.org/10.1016/j.desal.2008.05.113.

[26] Thomson M, Miranda M. Theory, testing and modelling of a Clark pump. CREST, Loughbrgh Univ Technol UK 2000;44:0–17.

[27] Thomson M, Miranda MS, Infield D. small scale SWRO system with excellent energy efficiency over a wide operating range.pdf. Desalination 2002;153:229–36.

[28] Desalination -Spectra | Home - Spectra n.d.

https://www.spectrawatermakers.com/us/us/products/desalination (accessed August 1, 2024).

[29] Mohamed ES, Papadakis G, Mathioulakis E, Belessiotis V. The effect of hydraulic energy recovery in a small sea water reverse osmosis desalination system; experimental and economical evaluation. Desalination 2005;184:241–6. https://doi.org/10.1016/j.desal.2005.02.066.

[30] Thomson M, Infield D. Laboratory demonstration of a photovoltaic-powered seawater reverse-osmosis system without batteries. Desalination 2005;183:105–11. https://doi.org/10.1016/j.desal.2005.03.031.

[31] Mohamed ES, Papadakis G, Mathioulakis E, Belessiotis V. An experimental comparative study of the technical and economic performance of a small reverse osmosis desalination system equipped with an hydraulic energy recovery unit. Desalination 2006;194:239–50. https://doi.org/10.1016/j.desal.2005.10.031.

[32] Manolakos D, Sh E, Karagiannis I, Papadakis G. Technical and economic comparison between PV-RO system and RO-Solar Rankine system . Case study : Thirasia island 2008;221:37–46. https://doi.org/10.1016/j.desal.2007.01.066.

[33] Bermudez-Contreras A, Thomson M. Modified operation of a small scale energy recovery device for seawater reverse osmosis. Desalin Water Treat 2010;13:195–202. https://doi.org/10.5004/dwt.2010.990.

[34] Dimitriou E, Mohamed ES, Karavas C. Experimental comparison of the performance of two reverse osmosis desalination units equipped with different energy recovery devices. Desalin. Environ. Clean Water Energy, 2014. https://doi.org/10.1080/19443994.2014.957935.

[35] Thomson M. Reverse-osmosis desalination of seawater powered by photovoltaics without batteries 2003.

[36] Heijman SGJ, Rabinovitch E, Bos F, Olthof N, van Dijk JC. Sustainable seawater desalination: Stand-alone small scale windmill and reverse osmosis system. Desalination 2009;248:114–7. https://doi.org/10.1016/J.DESAL.2008.05.045.

Declaration of interests

☒ The authors declare that they have no known competing financial interests or personal relationships that could have appeared to influence the work reported in this paper.

☐ The authors declare the following financial interests/personal relationships which may be considered as potential competing interests: